The N-terminal coiled-coil of Ndel1 is a regulated scaffold that recruits LIS1 to dynein

Eliza Żyłkiewicz,[1,2] Monika Kijańska,[1,2] Won-Chan Choi,[2] Urszula Derewenda,[2] Zygmunt S. Derewenda,[2] and P. Todd Stukenberg[1]

[1]Department of Biochemistry and Molecular Genetics and [2]Department of Molecular Physiology and Biological Physics, University of Virginia School of Medicine, Charlottesville, VA 22908

Ndel1 has been implicated in a variety of dynein-related processes, but its specific function is unclear. Here we describe an experimental approach to evaluate a role of Ndel1 in dynein-dependent microtubule self-organization using Ran-mediated asters in meiotic *Xenopus* egg extracts. We demonstrate that extracts depleted of Ndel1 are unable to form asters and that this defect can be rescued by the addition of recombinant N-terminal coiled-coil domain of Ndel1. Ndel1-dependent microtubule self-organization requires an interaction between Ndel1 and dynein, which is mediated by the dimerization fragment of the coiled-coil. Full rescue by the coiled-coil domain requires LIS1 binding, and increasing LIS1 concentration partly rescues aster formation, suggesting that Ndel1 is a recruitment factor for LIS1. The interactions between Ndel1 and its binding partners are positively regulated by phosphorylation of the unstructured C terminus. Together, our results provide important insights into how Ndel1 acts as a regulated scaffold to temporally and spatially regulate dynein.

Introduction

Cytoplasmic dynein is a complex, minus end–directed microtubule motor, involved in numerous cellular phenomena such as migration, organelle transport, and cell division. Dynein plays a critical role in the formation of the mitotic spindle, a microtubule-based machine that attaches chromosomes and divides them equally between daughter cells (Walczak and Heald, 2008). Dynein is required to anchor minus ends of spindle microtubules at the centrosomes (Goshima et al., 2005), and transports components of the spindle poles, such as NuMA (Merdes et al., 2000). Acentrosomal spindles can be self-organized in vitro by motors and microtubule-associated proteins (MAPs) around DNA-coated beads in meiotic *Xenopus* egg extracts, and they also require dynein to focus spindle poles (Vaisberg et al., 1993; Heald et al., 1996; Gaglio et al., 1997).

As might be expected based on its multifunctional nature, the cytoplasmic dynein complex is precisely regulated. Most of its functions in the cell require dynactin, another large, 1.2-MDa complex, which regulates cargo binding and processivity (Schroer, 2004). Other proteins are also involved, among them NudE and NudF, initially identified in the fungus *Aspergillus nidulans* as proteins required for nuclear migration (Efimov and Morris, 2000). Both NudE and NudF have homologues in vertebrate genomes with high amino acid sequence conservation: NudF is homologous to LIS1, which is mutated in a human genetic brain-malformation syndrome, lissencephaly (Xiang et al., 1995), whereas NudE is homologous to two mammalian paralogues, Nde1 and Ndel1, formerly known as NudE and NudEL, respectively (Feng et al., 2000; Niethammer et al., 2000; Sasaki et al., 2000). These two proteins share ∼55% amino acid identity, and each is made up of a long, parallel homodimeric coiled-coil that encompasses approximately the first 170 amino acids, followed by a C-terminal domain, which is thought to be largely unstructured, as inferred from the amino acid sequence analysis (Derewenda et al., 2007). The LIS1 protein, which is also a homodimer, made up of a small, N-terminal dimerization domain, followed by coiled-coil motif and a globular seven-blade

Correspondence to P. Todd Stukenberg: pts7h@virginia.edu

E. Żyłkiewicz was on leave from University of Warsaw, 00-927 Warsaw, Poland.

M. Kijańska was on leave from Technical University of Łódź, 90-131 Łódź, Poland.

M. Kijańska's present address is Insitute of Biochemistry, ETH Zurich, CH-8093 Zurich, Switzerland.

W.-C. Choi's present address is Korean Research Institute of Bioscience and Biotechnology, Yusong, Deajon 305-333, Korea.

Abbreviations used in this paper: CD, circular dichroism; CSF, cytostatic factor; DIC, dynein intermediate chain; MAP, microtubule-associated protein.

The Rockefeller University Press $30.00
J. Cell Biol. Vol. 192 No. 3 433–445
www.jcb.org/cgi/doi/10.1083/jcb.201011142

β-propeller domain (Kim et al., 2004; Tarricone et al., 2004; Mateja et al., 2006), binds to the coiled-coil domains of either Nde1 or Ndel1. The binding site was identified in Ndel1 as located approximately between residues 100 and 155 (Efimov and Morris, 2000; Feng et al., 2000; Derewenda et al., 2007). The putatively unstructured C-terminal domains of Nde1 and Ndel1 have been reported to have both functional and regulatory roles: they are implicated in interactions with dynein (Sasaki et al., 2000; Liang et al., 2004; Stehman et al., 2007) and contain regulatory phosphorylation sites (Stukenberg et al., 1997) for Cdk1 (Yan et al., 2003), Cdk5 (Niethammer et al., 2000), and Aurora A (Mori et al., 2007). The C-terminal domain is also believed to target Nde1 and Ndel1 to kinetochores during mitosis, where they recruit dynein, dynactin, and LIS1 (Liang et al., 2007; Stehman et al., 2007; Vergnolle and Taylor, 2007). Finally, Ndel1 has been shown to localize to the spindle poles in mitosis (Mori et al., 2007; Niethammer et al., 2000), where it is an important component in the assembly of the lamin B spindle matrix (Ma et al., 2009).

Relatively little is known about the nature and function of the tripartite complex consisting of dynein, LIS1, and Nde1/Ndel1. A recent elegant study demonstrated direct biochemical and biophysical evidence that Nde1 recruits LIS1 to form a stable interaction with dynein at a very specific point of its mechanochemical cycle (McKenney et al., 2010). In vitro, binding of both Nde1 and LIS1 to dynein induces a high load-bearing state of the motor, which might be critical for proper dynein function in such biological processes as translocation of chromosomes or organelles.

Despite of the significant body of work on Nde1/Ndel1 and their interacting partners, the precise molecular mechanisms by which these proteins function have been difficult to dissect in vivo due to the complexity of the system. Here, our goal was to identify an assay that isolates a specific function of Ndel1. We investigated the role of Ndel1 in the focusing of microtubule minus-ends into asters in extracts from *Xenopus* eggs arrested by the cytostatic factor (CSF) in meiosis, where microtubules are nucleated by constitutively active Ran^{Q69L} GTPase (Kalab et al., 1999; Ohba et al., 1999; Wilde and Zheng, 1999). This assay is independent of either kinetochores or centrosomes and serves as an important model of the self-organization of the meiotic spindle. The addition of Ran^{Q69L} to *Xenopus* egg extracts drives the formation of microtubules, and owing to the joint action of the motors and the MAPs, microtubules are assembled into asters with the minus ends focused toward a central point. Such oriented focusing of microtubules requires dynein (Heald et al., 1996; Gaglio et al., 1997; Walczak et al., 1998), which transports microtubule cross-linking proteins such as NuMA to the minus ends of microtubules (Merdes et al., 2000).

Here we show that asters cannot form after Ndel1 is removed by immunodepletion from meiotic *Xenopus* extracts, and that the addition of bacterially expressed coiled-coil fragment of mouse Ndel1 (residues 8–192), which includes both the dimerization motif and the LIS1-binding domain, is sufficient to restore the aster phenotype. We present evidence that this rescue depends on a hitherto undocumented and critically important interaction of the dimerization motif of Ndel1 with dynein. This interaction has two functions: it promotes microtubule bundling and allows Ndel1 to serve as a scaffold to recruit LIS1 to dynein. Further, mutants of Ndel1 that are defective in their ability to be phosphorylated by the Aurora A kinase (S251A) or Cdk1/Cdk5 kinases (T219A/T245A) cannot interact with dynein, suggesting that the unphosphorylated C-terminal domain sterically interferes with the Ndel1–dynein interaction.

Results

Ndel1 is the predominant paralogue in *Xenopus* eggs and embryos

The dissection of Nde1 and Ndel1 functions is complicated by the fact that it is not clear to what extent the expression of the two paralogues overlaps in different cell types (Stehman et al., 2007). To assess the levels of these proteins in *Xenopus* eggs, we generated polyclonal antibodies against both. After affinity purification using recombinant *Xenopus* Nde1 (xNde1) and Ndel1 (xNdel1), each antibody recognized 0.1 ng of its respective recombinant antigen (Fig. S1 a) but did not cross-react with the paralogue. The anti-xNdel1 antibody recognized a protein of ∼40 kD in immunoblots of *Xenopus* egg extracts (Fig. 1 a), whereas the anti-Nde1 antibody did not (Fig. S1 b). To test if xNde1 is developmentally regulated and absent in eggs, we harvested *Xenopus* embryos at the indicated stages of development and immunoblotted for xNde1 and xNdel1 (Fig. S1 c). We found that during early stages of development there are very low levels of xNde1, but they increase significantly before the onset of the mid-blastula transition, or stage 8 (Nieuwkoop and Faber, 1994). The knockdown of xNde1 in *Xenopus* embryos has previously been shown to generate brain defects (Feng et al., 2000) and interestingly the amount of xNde1 peaks at stages 10.5–15, which correspond to neurulation of the *Xenopus* embryo. In contrast, xNdel1 is detected throughout the development of the embryo, peaking at stage 15. This suggests that levels of xNde1 and xNdel1 are developmentally regulated, and that xNdel1 is the predominant protein in *Xenopus* eggs and early embryos. Consequently, the experiments described in this study relate primarily to xNdel1.

Ndel1 is required for microtubule aster formation in *Xenopus* egg extracts

Ran^{Q69L} was added to extracts to form Ran asters (Fig. 1 b) that were spun onto coverslips for visualization by immunofluorescence. *Xenopus* Ndel1 colocalized with dynein in the central focus of Ran asters (Fig. 1 c). To establish if the recruitment of xNdel1 is necessary for Ran-driven aster formation, we generated asters in the presence of an anti-xNdel1 antibody (Fig. 1, d and e). Although control extracts supplemented with rabbit IgG generated robust asters, only single microtubules or bundles were detected in the extracts in which Ndel1 was sequestered by an antibody. A similar phenotype was detected in extracts that contained an antibody against dynein intermediate chain (DIC) or p50/dynamitin, a dominant-negative inhibitor of dynactin (Fig. 1, d and e).

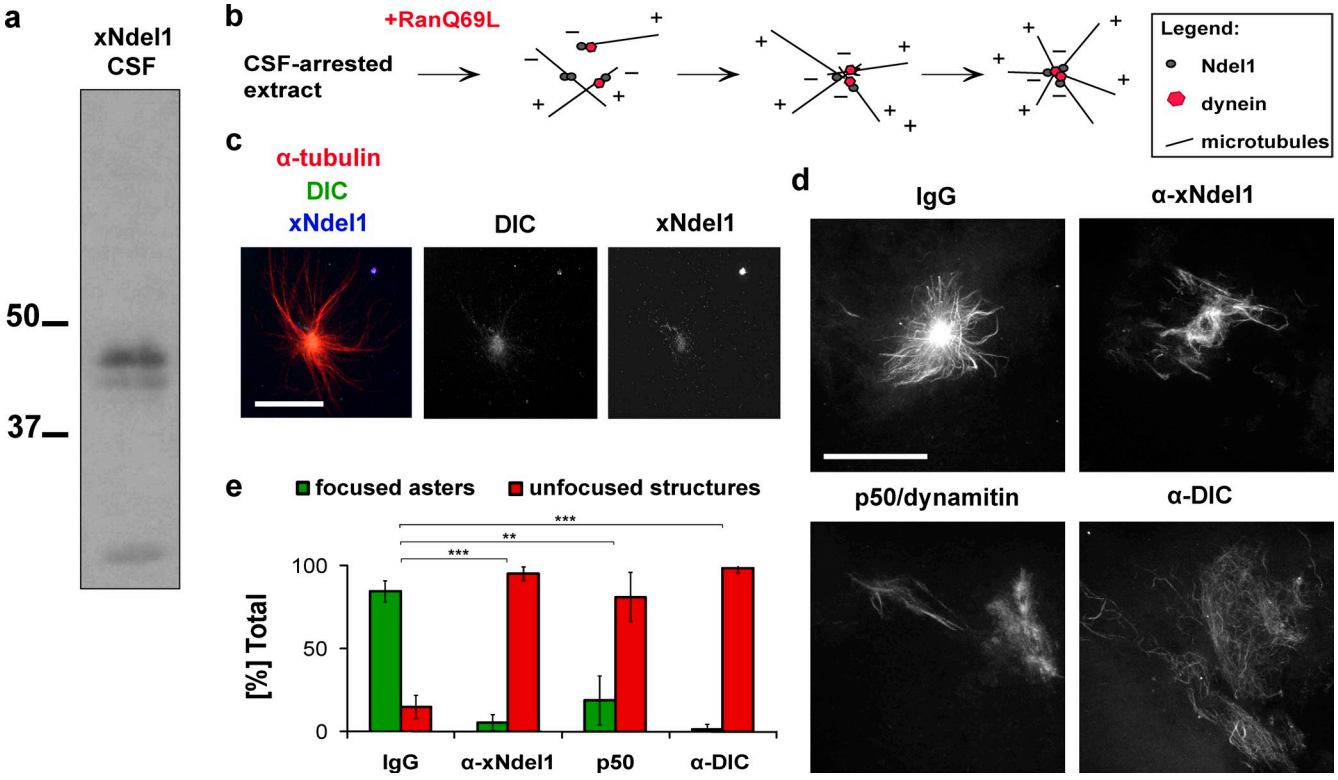

Figure 1. **Ndel1 function is required for microtubule aster formation.** (a) Affinity-purified α-Ndel1 antibodies recognize a 39-kD band in *Xenopus* egg extracts. (b) Schematic of putative role of dynein and Ndel1 in Ran aster formation in egg extracts. (c) Ndel1 colocalizes with dynein in the central focus of asters. (d) Addition of p50/dynamitin, α-dynein intermediate chain (DIC) or α-Ndel1 antibodies disrupts formation of microtubule asters. (e) Quantification of aster formation in the experiment described in panel d. Over 100 microtubule structures were quantified in three independent antibody addition experiments; asterisks indicate statistically significant differences (Student's *t* test with $P < 0.05$; ** indicates $P < 0.005$; *** indicates $P < 0.0005$). Bar, 20 µm.

Because aster formation could be blocked either by inhibition of tubulin polymerization into microtubules or failure of microtubules to organize into an aster, we compared the amount of microtubules generated in extracts containing Ran^{Q69L} in the presence or absence of anti-xNdel1 antibodies. In both experiments we found similar amounts of tubulin pelleted through glycerol cushions, demonstrating that microtubule polymerization is not impaired (Fig. S2 a). We conclude that Ndel1 is not involved in microtubule assembly, but is essential for microtubule self-organization into asters.

Next we tested whether Ndel1 has a general function in focusing microtubules, by generating microtubules in *Xenopus* extracts by the addition of DMSO. Although DMSO could stabilize microtubules in extracts with or without Ndel1 antibodies, only extracts containing Ndel1 function could focus those microtubules into asters. In extracts compromised for Ndel1 function, we could only detect arrays of unfocused microtubules (Fig. S2 b, quantified in c).

Ndel1's coiled-coil domain is necessary and sufficient for aster formation

We assayed aster formation in egg extracts from which xNdel1 was immunodepleted before addition of Ran^{Q69L}. After depletion of over 90% of xNdel1 (Fig. 2 b), extracts could not assemble asters. Instead, we observed bundles of disorganized microtubules or single microtubules (Fig. 2 b′). To verify if the loss of the microtubule focusing into asters was directly caused by the removal of xNdel1, we conducted a rescue assay in which we supplemented immunodepleted extracts with recombinant Ndel1 proteins (Fig. 2, b′ and b′′). Given that a crystal structure of the mouse Ndel1 coiled-coil domain is known (Derewenda et al., 2007), and that it is 81% identical with respect to the amino acid sequence to the *Xenopus* protein, we decided to use recombinant mouse Ndel1 (mNdel1, Fig. S3 a). We reasoned that this approach would enable us to rationally design structure-based mutations without disrupting structural features of the protein. The construct used, encompassing residues 8–310, was the longest polypeptide chain that could be expressed and purified from *Escherichia coli* without noticeable degradation (Fig. S3 a). It contains the entire coiled-coil domain and most of the C-terminal domain (Fig. 2 a), but lacks the N-terminal eight residues that have no known biological function, and 35 amino acids at the C terminus. Recent data show that the C terminus downstream of glycine 315 is variable due to alternative splicing (Bradshaw et al., 2009), so the $mNdel^{8–310}$ fragment should be fully representative of the biologically active protein. To determine if recombinant mouse protein can rescue xNdel1 depletion we used 100 nM mNdel1, which is the estimated concentration of xNdel1 in *Xenopus* egg extracts (Ma et al., 2009). When extracts immunodepleted of xNdel1 were supplemented with $mNdel1^{8–310}$, aster formation was fully restored (Fig. 2, b′ and b′′).

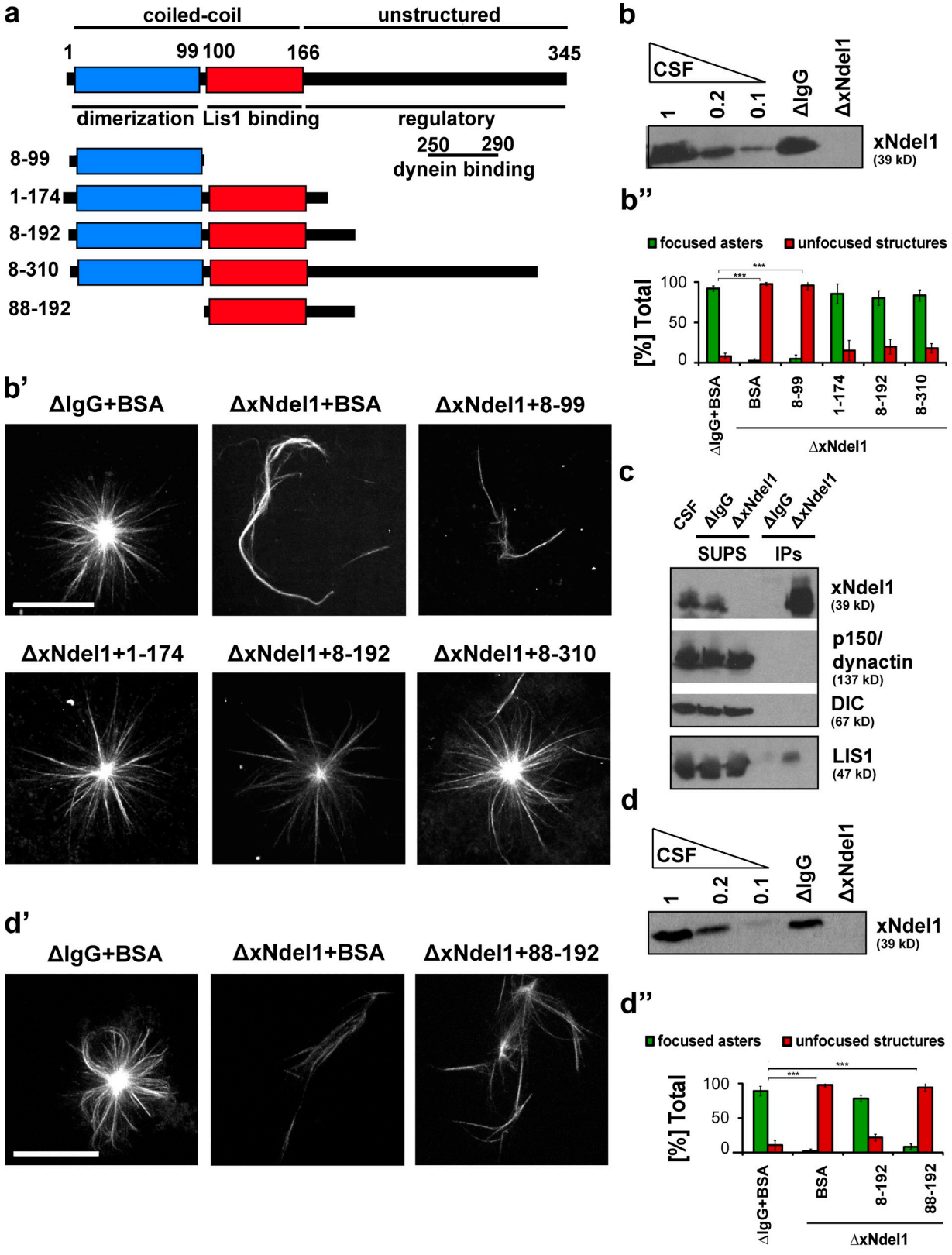

Figure 2. **The entire N-terminal coiled-coil of Ndel1, but not the LIS1-binding domain alone, is sufficient to rescue microtubule aster formation in *Xenopus* egg extracts.** (a) Schematic of truncated mouse Ndel1 (mNdel1) proteins used in rescue experiments. (b) Ndel1 proteins were immunodepleted greater than 90%. CSF-arrested extracts were diluted to the specified amount or control ΔIgG and ΔxNdel1 extracts were immunoblotted with affinity-purified polyclonal α-Ndel1 antibodies. (b′) Representative images of the predominant microtubule structures observed after rescuing xNdel1-depleted extracts (ΔxNdel1) with the indicated recombinant proteins. Structures such as those in ΔxNdel1+1–174 (mNdel1$^{1–174}$), ΔxNdel1+8–192 (mNdel1$^{8–192}$), and ΔNdel1+8–310 (mNdel1$^{8–310}$) would be classified as asters, whereas those seen in ΔxNdel1+BSA and ΔxNdel1+8–99 (mNdel1$^{8–99}$) are unfocused structures. (b′′) Quantification of three independent experiments after Ndel1 depletion and rescue with truncated mouse Ndel1 proteins; for each depletion and rescue condition over

We also tested if the recombinant protein affected aster formation in control extracts by adding 100 nM Ndel1$^{8–310}$ to nondepleted extracts. There was no dominant-negative effect (Fig. S4, a and b).

Next, we asked if Ndel1 alone is responsible for the phenotype, or if the immunodepletion also removes LIS1 from the extracts, as might be expected due to the interaction between the two proteins (Efimov and Morris, 2000; Niethammer et al., 2000; Sasaki et al., 2000; Smith et al., 2000; Liang et al., 2004; Derewenda et al., 2007; Stehman et al., 2007). We analyzed the immunoprecipitates and immunodepleted extracts by Western blot (Fig. 2 c). Although a small amount of LIS1 was indeed detected in the xNdel1 immunoprecipitates, most of it remained in the extract, even though xNdel1 was depleted below the detection level. We conclude that xNdel1 depletion does not remove LIS1 to a degree that could compromise its independent function (Fig. 2). Consequently, xNdel1 is specifically required to organize microtubules into asters in *Xenopus* egg extracts, whereas LIS1 in physiological concentrations is not sufficient to sustain a normal phenotype.

We asked which structural domains are critical for aster formation. Guided by the crystal structure of the coiled-coil domain of mNdel1 (Derewenda et al., 2007), we designed and expressed a series of truncated mNdel1 variants (Fig. 2 a) and tested their ability to rescue aster formation in xNdel1-depleted extracts (Fig. 2, b′ and b′′). Surprisingly, the mNdel1$^{8–192}$ fragment, which lacks the C-terminal domain containing a putative dynein-binding site (Sasaki et al., 2000; Liang et al., 2004), was fully able to rescue aster formation, as was an even shorter fragment, mNdel1$^{1–174}$ (Fig. 2, b′ and b′′). Thus, the coiled-coil fragment is the minimum domain of Ndel1 functional in microtubule self-organization into asters.

The coiled-coil fragment of Ndel1 is organized into two distinct structural elements (Fig. 2 a). Residues 8–99 form a tightly associated parallel coiled-coil that is responsible for the homodimerization of the protein. Residues 100–166 are able to associate into a coiled-coil with much lower affinity, and can interact with an analogous fragment from another Ndel1 molecule to generate an antiparallel four-helix bundle, and effectively a dimer of dimers. This latter fragment is highly conserved between Nde1 and Ndel1, and contains the LIS1-binding epitope (Derewenda et al., 2007). A recombinant mNdel1 variant lacking this portion of the coiled-coil (mNdel1$^{8–99}$) is unable to generate asters (Fig. 2, b′ and b′′).

We also tested if the LIS1-binding fragment alone, mNdel1$^{88–192}$, could rescue aster formation in a similar experiment and found that this protein did not rescue aster focusing (Fig. 2, d′ and d′′). Thus, the entire coiled-coil domain of Ndel1, which includes both the dimerization domain and the LIS1-binding motif, is required to organize microtubules into asters. None of the coiled-coil fragments displayed a dominant-negative effect after addition to nondepleted extracts (Fig. S4, a and b).

A novel dynein-binding site on the coiled-coil of Ndel1 is critical for aster formation

We were surprised that truncated variants of Ndel1 lacking the established dynein-binding domain in the C terminus could rescue aster formation, and wondered if there was a second dynein-binding site on the coiled-coil. To address that possibility, purified recombinant mNdel1 proteins were covalently coupled to Sepharose beads at a final concentration of 30 µM, incubated in meiotically arrested *Xenopus* egg extracts, and extensively washed with salt. Dynein and LIS1 were then identified by immunoblotting with antibodies against the DIC and LIS1, respectively (Fig. 3 a). Only Ndel1 proteins containing the LIS1-binding motif pulled down LIS1. All Ndel1 variants that contained residues 8–99 (the dimerization motif) pulled down dynein. The mNdel1$^{8–310}$ variant, which contains the established dynein-binding site, did not bind appreciably more dynein than any of the variants that contained residues 8–99. The mNdel1$^{88–192}$ variant pulled down LIS1 but not dynein, demonstrating that the interaction sites for dynein and LIS1 do not overlap. We tested if this novel dynein-binding motif was also found on Nde1. We found that beads containing 30 µM of two N-terminal fragments of Nde1 pulled down similar amounts of dynein as the Ndel1 (Fig. 4 a). In addition, similarly to Ndel1$^{88–192}$, Nde1$^{89–174}$ pulled down LIS1, but not dynein (Fig. 4 a).

To further dissect the novel Ndel1–dynein interaction mechanism, we identified specific amino acids on Ndel1 that are involved in binding of dynein. We noted that dynein can be washed off the mNdel1-conjugated beads with 0.5–0.75 M NaCl (Fig. S5 a), suggesting that the interaction between Ndel1 and dynein may be largely electrostatic in nature. The dimerization fragment of Ndel1 contains multiple conserved polar amino acids, mostly glutamates. We designed double mutants of mNdel1$^{8–192}$, i.e., E36A/E39A and E48A/E52A (Fig. 3 b). These variants were expressed in *E. coli* and purified. Circular dichroism (CD) spectra were recorded to ensure that mutations do not affect the folding of these proteins into coiled-coils. We found that mNdel1$^{8–192\ (E36A/E39A)}$ and mNdel1$^{8–192\ (E48A/E52A)}$ have very similar spectra as the wild type, suggesting that they are properly folded (Fig. S3 b). We performed pull-down experiments with *Xenopus* extracts, using the two variants as bait, and determined that they were impaired in dynein binding. The mNdel1$^{8–192\ (E36A/E39A)}$ protein reduced binding and the interaction was below the level of detection in mNdel1$^{8–192\ (E48A/E52A)}$ (Fig. 3 c). To compare the relative amounts of dynein binding

100 microtubule structures were quantified; asterisks indicate statistically significant differences (Student's *t* test with $P < 0.05$; *** indicates $P < 0.0005$). (c) Ndel1 coimmunoprecipitates LIS1, but not dynein and dynactin in *Xenopus* egg extracts, and α-Ndel1 antibodies do not deplete LIS1. α-Ndel1 antibodies were used to immunoprecipitate proteins from *Xenopus* CSF-arrested extracts. The resulting precipitates (IPs) and extracts from which the IP was performed (SUPS) were immunoblotted for indicated proteins. (d) Level of Ndel1 depletion from CSF-arrested egg extract as measured by immunoblot. (d′) LIS1-binding domain mNdel1$^{88–192}$ (88–192) is not sufficient to rescue aster formation in Ndel1-depleted extracts. (d′′) Quantification of microtubule structures from three independent experiments where Ndel1-depleted extracts were rescued with the indicated mNdel1 variants. Over 100 microtubule structures were quantified, asterisks indicate statistically significant differences (Student's *t* test with $P < 0.05$; *** indicates $P < 0.0005$). Bar, 20 µm.

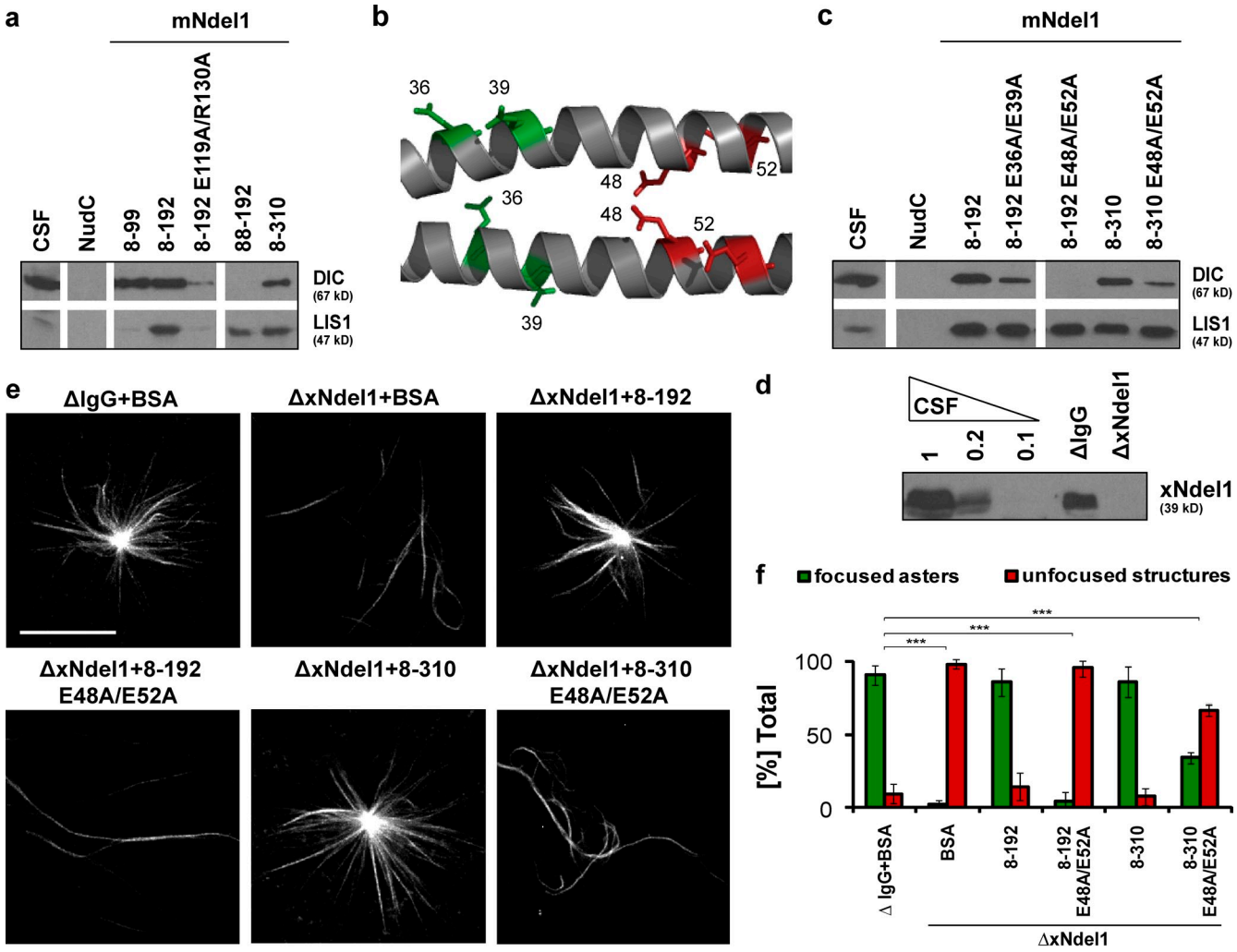

Figure 3. **Dynein interacts with polar residues within the coiled-coil domain of Ndel1.** (a) Immunoblot analysis of dynein IC (DIC) and LIS1 pulled down from CSF-arrested *Xenopus* egg extract by the indicated recombinant mouse Ndel1 proteins. (b) Multiple conserved glutamic acids extend form the coiled-coil backbone of Ndel1; residues shown in color were mutated, residues shown in red are the most critical for dynein binding; image created in Pymol (http://www.pymol.org/) based on the structure of mNdel1$^{8–192}$ (Protein Data Bank accession no. 2v71). (c) Immunoblot analysis of dynein IC (DIC) and LIS1 pulled down from mitotic *Xenopus* egg extract by mutated mNdel1$^{8–192}$ and mNdel1$^{8–310}$ proteins. (d) Level of Ndel1 depletion from CSF-arrested egg extract with affinity-purified polyclonal α-Ndel1 antibodies analyzed by Western blot. (e) mNdel1$^{8–192\ E48A/E52A}$ (8–192 E48A/E52A) and mNdel1$^{8–310\ E48A/E52A}$ (8–310 E48A/E52A) proteins do not significantly rescue aster formation. Representative images of predominant phenotypes from each condition are shown. (f) Quantification of over 100 microtubule structures from three independent experiments after Ndel1 depletion and rescue with mouse Ndel1 variants; asterisks indicate statistically significant differences (Student's *t* test with $P < 0.05$; *** indicates $P < 0.0005$). Bar, 20 µm.

in the two sites on Ndel1 we mutated glutamates 48 and 52 to alanines in mNdel1$^{8–310}$, a variant that contains the C-terminal dynein-binding site. In this case we repeatedly detected low levels of dynein binding, suggesting that the C-terminal site binds dynein with lower affinity than the novel N-terminal site.

Next, we tested if mNdel1$^{8–192\ (E36A/E39A)}$, mNdel1$^{8–192\ (E48A/E52A)}$, and mNdel1$^{8–310\ (E48A/E52A)}$ could rescue Ran-induced aster formation in xNdel1-depleted *Xenopus* egg extracts. We added these proteins to nondepleted extracts and found that aster formation was not affected (Fig. S4, a and b). Extracts depleted of endogenous Ndel1 and containing mNdel1$^{8–192\ (E36A/E39A)}$ could rescue ∼70% of aster focusing, whereas mNdel1$^{8–192\ (E48A/E52A)}$ only generated disorganized microtubule structures (Fig. S5, b and c; Fig. 3, e and f). mNdel1$^{8–310\ (E48A/E52A)}$, which contains only the C-terminal dynein-binding site, generated mostly unfocused structures, although 35% of microtubule bundles were focused into asters. Thus, the ability of Ndel1's coiled-coil to bind dynein via its dimerization motif correlates strongly to its potential to generate focused asters in *Xenopus* egg extracts.

The dynein-binding function is conserved in Nde1

Not surprisingly, the coiled-coil of Nde1 can bind dynein in a pull-down assay, just like Ndel1 (Fig. 4 a). Therefore, we tested if it could also function in aster formation. We depleted *Xenopus* egg extracts of xNdel1 and rescued with either mNde1$^{7–99}$ or mNde1$^{7–170}$ (Fig. 4, c and d). In a manner similar to corresponding fragments of Ndel1, mNde1$^{7–170}$ fully rescued aster formation, whereas mNdel1$^{7–99}$ failed to do so. These data argue that coiled-coils of Nde1 and Ndel1 are capable of similar activities in dynein regulation.

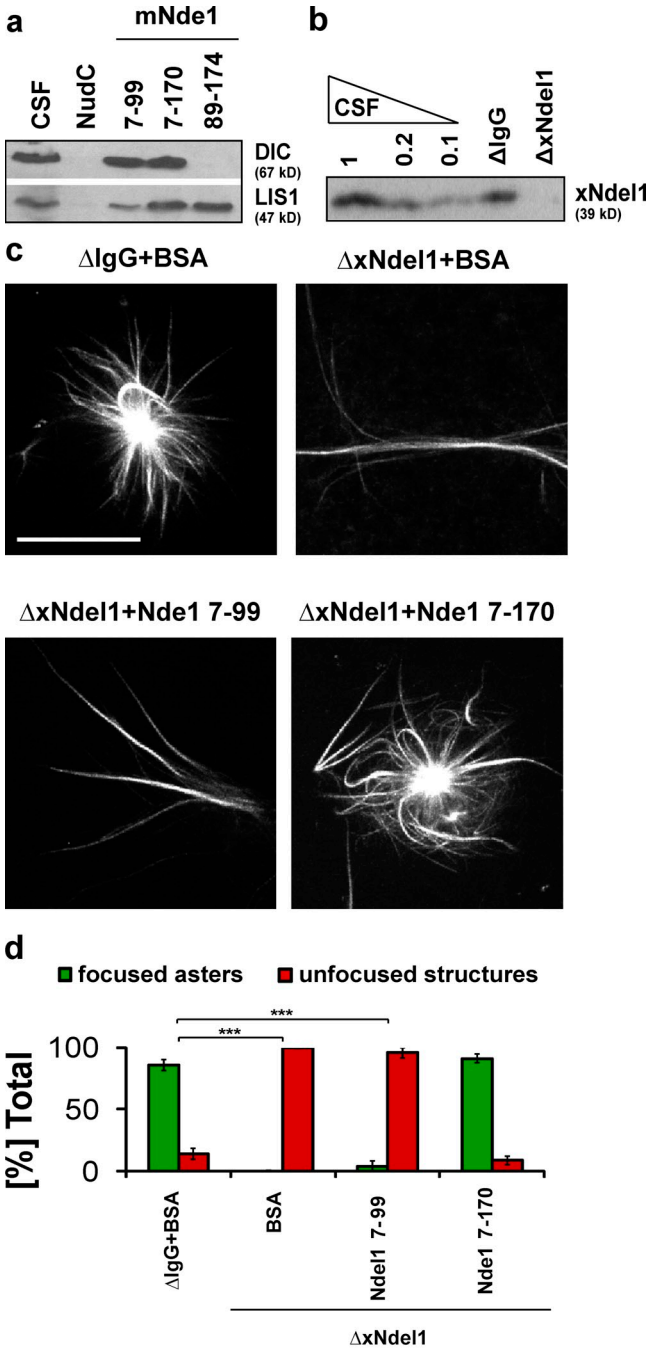

Figure 4. **The N terminus of Nde1 can focus microtubules into asters.** (a) Immunoblot analysis of dynein IC (DIC) and LIS1 pulled down from CSF-arrested *Xenopus* egg extract by the indicated recombinant mouse Nde1 proteins. (b) Level of Ndel1 depletion from CSF-arrested egg extracts with affinity-purified polyclonal α-Ndel1 antibody analyzed by Western blot. (c) Addition of mNde1$^{7–170}$ to xNdel1-depleted extracts rescues aster formation. (d) Quantification of microtubule structures from three independent experiments where Ndel1-depleted extracts were rescued with the indicated mouse Nde1 variants; over 100 microtubule structures were quantified from each experiment; asterisks indicate statistically significant differences (Student's *t* test with $P < 0.05$; *** indicates $P < 0.0005$). Bar, 20 µm.

Ndel1 is a scaffold that recruits LIS1 to dynein

We determined that the recruitment of LIS1 via the coiled-coil domain is important for Ndel1 function in aster formation (Fig. 2, d′ and d′′). We generated a double-point variant of mNdel1$^{8–192(E119A/R130A)}$, which lacks two side chains essential for the interaction between Ndel1 and LIS1 (Derewenda et al., 2007). The mutant could not pull down LIS1 from *Xenopus* extracts (Fig. 3 a), and it did not rescue aster focusing in xNdel1-depleted extracts (Fig. 5, b and c). However, we observed very robust bundling of microtubules (scored as bundles; Fig. 5, b and c) that was not observed in xNdel1-depleted extracts or extracts rescued with variants lacking either the dimerization domain or the LIS1-binding region (Fig. 2). These data suggest that when Ndel1 bound dynein, but not LIS1, it generated bundled microtubules, although it could not organize them enough to form asters. Alternatively, LIS1 binding to Ndel1 may inhibit this bundling activity.

Ndel1 has two distinct binding sites on its coiled-coil, which independently bind dynein and LIS1, suggesting that the coiled-coil acts as a scaffold. Scaffolds can significantly increase the effective local concentrations of proteins by providing a bridging function. To test if Ndel1 follows this paradigm, we asked if adding excess of LIS1 to xNdel1-depleted extracts induced aster formation. Extracts containing an additional 350 nM LIS1 produced focused microtubule structures, although the asters were usually smaller and could only be produced 35% of the time. Approximately 30% of the microtubule structures in these extracts contained multiple bright foci reminiscent of aster centers, but the microtubules surrounding these foci were not organized (scored as multiple foci; Fig. 5, b and c). We conclude that LIS1 can focus microtubules in the absence of Ndel1, demonstrating that LIS1 is downstream of Ndel1. Moreover, the results support the model that Ndel1 recruits LIS1 to the dynein complex.

Both the coiled-coil of Ndel1 and LIS1 appear to have distinct effects in the aster assay. The Ndel1 variant that cannot bind LIS1 generated cross-linked microtubule bundles, whereas exogenous LIS1 yielded arrays of microtubules with multiple foci. To determine if the two proteins interact independently, we combined mNdel1$^{8–192(E119A/R130A)}$ and 350 nM LIS1. Aster formation was largely restored; however, we also observed a small percentage of distorted asters with hollow centers (Fig. 5 d). Therefore, we conclude that Ndel1 may have a LIS1-independent function in regulating dynein.

Because Ndel1 likely acts as a recruitment factor for LIS1, disrupting the balance of Ndel1 and LIS1 should affect aster formation. Indeed, aster focusing was affected when LIS1 alone, or in combination with Ndel1$^{8–192\ (E119A/R130A)}$, was added to non-depleted *Xenopus* egg extracts (Fig. S4, a and b).

The C-terminal domain of Ndel1 negatively regulates its interaction with dynein

The C termini of Ndel1 and Nde1 are fairly divergent, but also similar in that they contain a number of phosphorylation sites and have the potential to bind regulatory proteins. It is unclear, however, how these domains regulate Nde1/Ndel1 function. We hypothesized that phosphorylation may provide a regulatory mechanism for dynein binding, so that the unphosphorylated protein is autoinhibited. To test if phosphorylation of the C terminus in Ndel1 activates the dynein-binding site on the

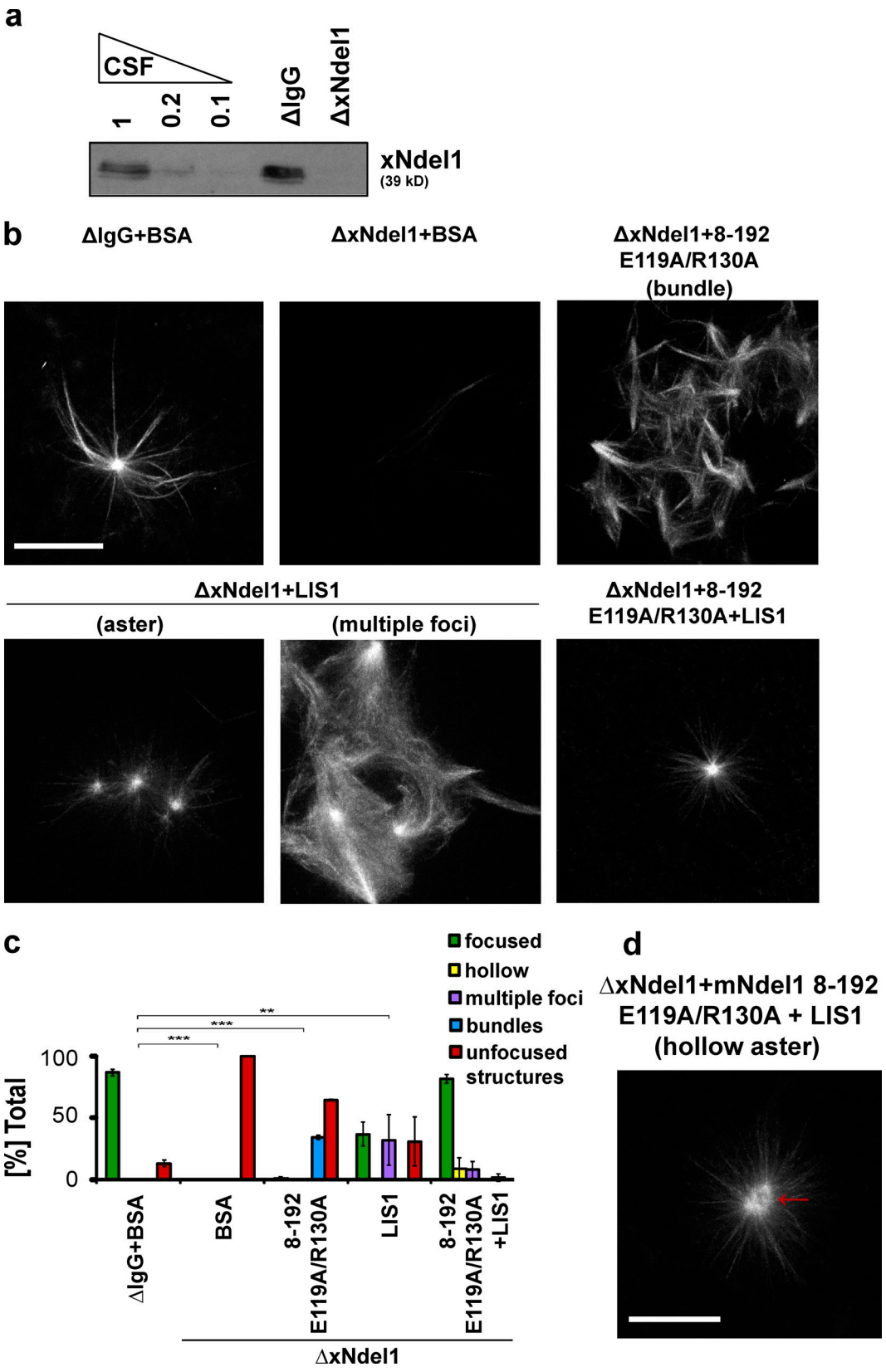

Figure 5. **Ndel1 recruits LIS1 to drive aster formation, and a mutant that cannot bind LIS1 generates microtubule bundles.** (a) Depletion level quantification for experiment shown in panel d. (b) The role of Ndel1 is to recruit LIS1 to drive aster formation. The interaction between LIS1 and Ndel1 is required for aster formation, but Ndel1 also has a LIS1-independent function. Representative images of the predominant microtubule structures assembled in Ndel1-depleted extracts rescued with the indicated recombinant protein(s). Note that the Ndel1 proteins with mutated LIS1-binding residues are unable to form asters, but the resulting structures are more organized than in Ndel1-depleted extracts (bundles). Addition of 350 nM exogenous LIS1 to Ndel1-depleted extracts partly rescues microtubule focusing, whereas addition of 350 nM LIS1 and 100 nM Ndel1$^{8–192\ E119A/R130A}$ (8–192 E119A/R130A) rescues significantly better.

coiled-coil, we generated two mNdel1 variants with point mutations at previously characterized phosphorylation sites: mNdel1$^{8–310\ (S251A)}$, a single site mutant deficient in its susceptibility to Aurora A (Mori et al., 2007), and a double mutant, mNdel1$^{8–310\ (T219A/T245A)}$, which lacks two sites phosphorylated by Cdk1 and Cdk5 (Niethammer et al., 2000; Yan et al., 2003). These recombinant proteins were used as bait in pull-down experiments with *Xenopus* egg extracts (Fig. 6 a). Compared with the wild-type mNdel1$^{8–310}$, mNdel1$^{8–310\ (S251A)}$ and mNdel1$^{8–310\ (S219A/T245A)}$ pulled down almost no dynein.

Discussion

The scaffold function of the coiled-coil domain of Ndel1

When Ndel1 is immunodepleted from egg extracts, microtubule asters cannot be formed by constitutively active Ran. This phenotype is similar to that seen after disrupting functions of dynein (Ohba et al., 1999) or dynactin (Wittmann and Hyman, 1999), suggesting that Ndel1 immunodepletion interferes with a dynein-dependent pathway required in the self-organization of microtubules into asters. The N-terminal coiled-coil domain of mNdel1, residues 8–192 or 1–174, was sufficient to rescue aster formation. This was surprising because this region of Ndel1 lacks the previously characterized dynein-binding motif, located within the C-terminal portion of Ndel1 (Sasaki et al., 2000; Liang et al., 2004). Subsequently, we showed that mNdel1$^{8–192}$ contained a second dynein-binding site, spanning residues 36–52, and we demonstrated that this interaction is critical for dynein to function in the formation of Ran asters. The paralogue Nde1 also interacts with dynein in vitro via this motif, suggesting a common function. The N-terminal interaction with dynein is also independent of LIS1, and increasing the concentration of LIS1 in extracts can partially rescue the depletion of Ndel1. Together these data suggest that Ndel1 (and Nde1 in relevant cells) serves as molecular scaffold that binds dynein, and at the same time recruits LIS1 to the motor. Such a mechanism is strongly supported by recent single-molecule biophysical studies on the role of LIS1 and Nde1 in dynein function (McKenney et al., 2010).

Our studies have also identified a possible LIS1-independent role of Ndel1. The mNdel1$^{8–192\ (E119A/R130A)}$ mutant, which is unable to bind LIS1, still leads to cross-linked microtubule bundles that were not seen in mNdel1-depleted extracts. Similarly, although exogenous recombinant LIS1 in concentrations exceeding physiological levels delivers a partial rescue for Ndel1 depletion in aster focusing, this concentration is sufficient for focusing in extracts that also contain mNdel1$^{8–192\ (E119A/R130A)}$. These data argue either that LIS1 at additional 0.5x concentration (Wang and Zheng, 2011) now binds mNdel1$^{8–192\ (E119A/R130A)}$, or that there is a LIS1-independent function of Ndel1. We prefer the latter scenario, as it is unlikely that mNdel1$^{8–192\ (E119A/R130A)}$ can still bind LIS1. We have combined two different mutations, which independently inhibit binding in vitro (Derewenda et al., 2007; Wang and Zheng, 2011), and show that the resulting mutant could not pull down LIS1 from extracts. Thus, we think it likely that both proteins act independently of one another when in isolation, and their interaction amplifies and modulates those activities. The LIS1-independent activity of Ndel1 is an important avenue for future research.

The regulation of Ndel1–dynein interaction via phosphorylation

Our studies also provide insight into how Ndel1 is regulated. The C-terminal domains of Ndel1/Nde1 are known to undergo phosphorylation by several different kinases (Stukenberg et al., 1997; Niethammer et al., 2000; Yan et al., 2003; Mori et al., 2007, 2009), suggesting that it regulates function of Ndel1. However, the molecular consequences of these phosphorylations were not understood. We determined that the interaction between the N-terminal site on Ndel1 and dynein is inhibited until the C-terminal domain is properly phosphorylated. Specifically, mNdel1$^{8–310}$ variants with abrogated phosphorylation sites (i.e., T219A and T245A or S251A) do not bind dynein. In our assays we used *Xenopus* extracts that are able to generate bipolar spindles that segregate chromosomes, which strongly argues that they contain all the required mitotic regulators. Thus, when we put the unphosphorylated proteins on beads into these extracts, they can undergo full phosphorylation to uncover the dynein-binding site.

Consistent with a model that the C terminus blocks the N-terminal binding site, the pI of the C-terminal fragment encompassing residues 180–345 is 9.8, whereas the pI of the N-terminal dimerization motif of Ndel1 is 4.6. Thus, there would be a considerable electrostatic attraction between these two fragments when aligned side by side (Fig. 6 b, bottom). Phosphorylation would introduce negative charges and lead to the electrostatic expulsion of the C-terminal domain. This is a plausible mechanism, but for a dimeric Ndel1 it implies that the C-terminal domain must fold back ∼150 Å in a jackknife manner to achieve the autoinhibited conformation. Given that the C terminus is predicted to be mostly unstructured, such a dramatic conformational change is possible in principle, but is unlikely because it would be entropically unfavorable. A possible alternative explanation is offered by the crystal structures of two different fragments of the Ndel1 coiled-coil (Derewenda et al., 2007). This study revealed that Ndel1 has a propensity to form an antiparallel dimer of dimers, mediated by a fragment encompassing residues 100–165. In the tetramer the C terminus would extend in an antiparallel fashion along the coiled-coil of the adjacent dimer (Fig. 6 b, top). It is currently a matter of debate whether Ndel1 is a tetramer when not bound to dynein. Solution studies have shown that a dimer was the

(c) Quantification of microtubule structures from three independent experiments where Ndel1-depleted extracts were rescued with the indicated mouse Ndel1 proteins and/or LIS1; over 100 microtubule structures were quantified; asterisks indicate statistically significant differences in percentage of focused asters (Student's *t* test with $P < 0.05$; ** indicates $P < 0.005$; *** indicates $P < 0.0005$). (d) Representative image of a hollow aster. Image is shown at different contrast than in panel b to emphasize presence of a hollow center of the aster. Bar, 20 µm.

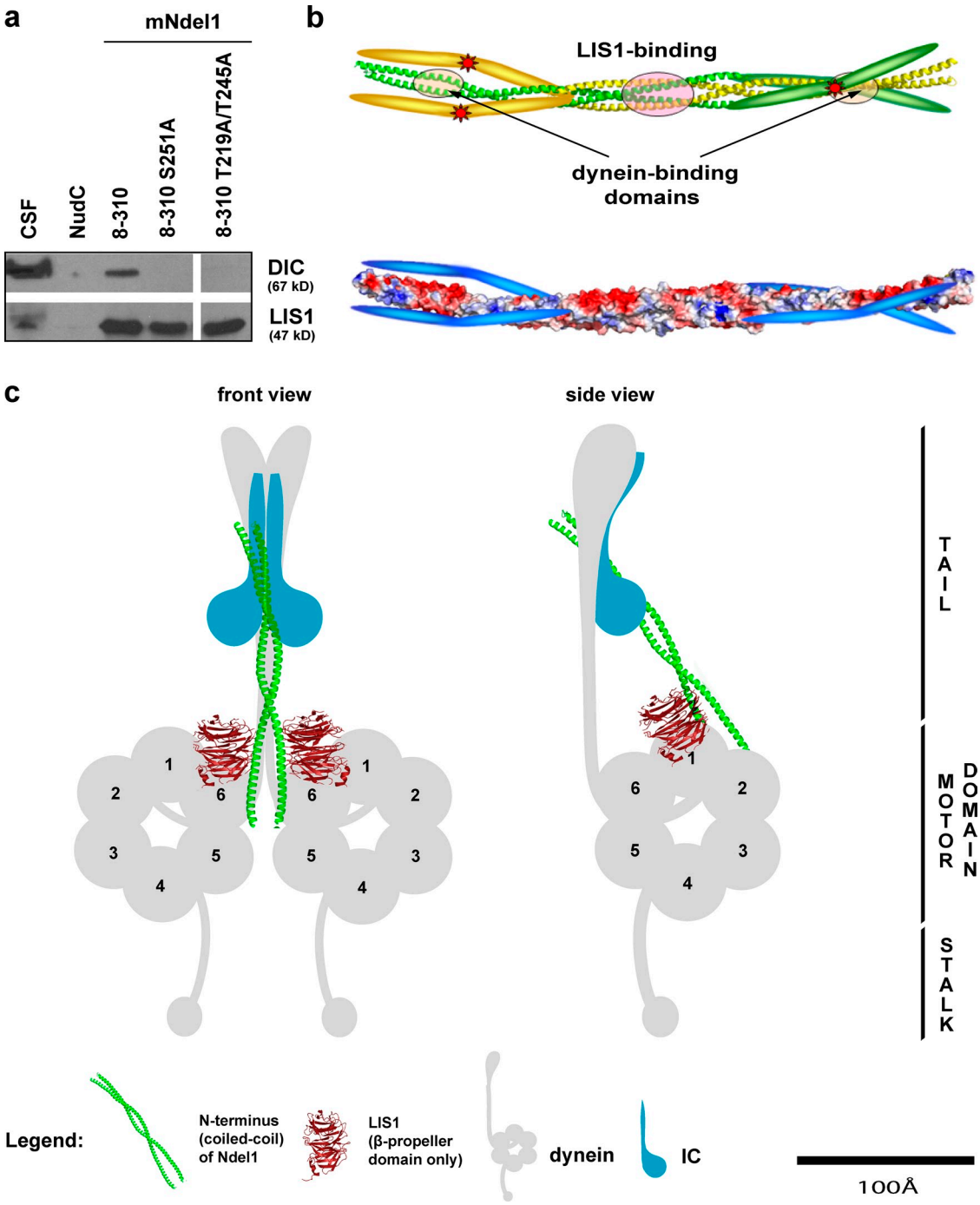

Figure 6. **Proposed role for the regulation of Ndel1 ability to act as a scaffold to promote the interaction between dynein and LIS1.** (a) Ndel1 mutants in Aurora A consensus site (S251A) and Cdk1/Cdk5 sites (T219 and T245) abolish the interaction with dynein in a pull-down assay. (b, top) A ribbon model of a nascent Ndel1 tetramer where one dimeric coiled-coil is green and the second is yellow. Note that the structure of the C terminus has not been solved and is presented in cartoon format. The asterisks indicate potential phosphorylation sites. (b, bottom) Space-filling model colored to show charge distribution of Ndel1 in the presumptive autoinhibited form. The C terminus has a pI of 9.8 and is therefore depicted schematically as blue. We propose that in the unphosphorylated state the two Ndel1 dimers interact through the LIS1-binding region, as seen in the crystal structure. In this conformation the highly basic C-terminal tail inhibits the interaction between Ndel1 and dynein by binding the highly acidic (pI 4.5) dynein interaction region on the coiled-coil as shown. (c) Proposed model of the tripartite interaction between dynein, LIS1, and the N terminus of Ndel1. The proteins are all drawn approximately to scale, although their precise locations are not known.

predominant species for the mNdel1$^{8–192}$ variant in vitro. However, a more recent study reported data from COS7 cells that support the notion of Ndel1 tetramerization in vivo (Collins et al., 2008). It is therefore possible that the pool of autoinhibited Ndel1/Nde1 exists in cells as tetramers, or more precisely dimers-of-dimers.

Model of the tripartite Ndel1–LIS1–dynein interaction

Both Ndel1 and LIS1 are homodimers, and they interact to form a heterotetramer with intrinsic symmetry (Derewenda et al., 2007) that would mirror the symmetry of the homodimeric

dynein complex. Such a stoichiometry strongly suggests that the Ndel1–LIS1 complex would bind centrally between the two motor domains of dynein (Fig. 6 c).

LIS1 binds the AAA1 site of the dynein motor domain (Sasaki et al., 2000; Tai et al., 2002; McKenney et al., 2010), and very recent data suggest that the coiled-coil of Ndel1 interacts with two identical intermediate chain (IC) subunits on the cargo-binding tail of dynein (Wang and Zheng, 2011). The ICs are scaffolds in their N-terminal ends that bind several dynein light and light intermediate chains, and contain a WD40 (β-propeller) domain in their C termini. Based on structural considerations, we speculate here that the Ndel1 coiled-coil is likely to bind between the two β-propeller domains of IC, in a manner similar to its interaction with LIS1. Thus, the scaffold function would involve two similar interactions of a coiled-coil with WD40 dimers, located ∼90Å apart. The unstructured C-terminal fragment of Ndel1 can potentially reach its putative target, IC or LC8 within the tail of dynein and not far from the IC WD40 domain (Stehman et al., 2007). This leads to an interesting model in which the tail and motor domains of dynein are cross-linked by Ndel1/Nde1 to coordinate the two motor domains, so that at any time LIS1 interacts with one motor domain in the pre-powerstroke state to regulate force production (McKenney et al., 2010). The microtubule-releasing activity of dynein could be regulated by Ndel1 to prevent nonprocessive stalling of the motor on microtubules, as suggested in a recent paper (McKenney et al., 2010).

The model we present is consistent with published experimental data and also with the cryo-EM data for dynein (Burgess et al., 2003; Mizuno et al., 2007). The AAA1 fragment of the motor domain of dynein appears to be close enough to the tail to make a distance of ∼100 Å for the proposed interaction quite feasible. To our knowledge, our model for the first time suggests a cross-linking mechanism between the motor and tail domains. It will be interesting to see if this architecture is maintained throughout the entire cycle, or if it locks the tails only at a specific point.

Materials and methods

Isolation of Nde1 and Ndel1 clones

Full-length *Xenopus* Nde1 (MP43) was cloned into pET 30 vector (EMD) from pCS2+ vector (Stukenberg et al., 1997) through NcoI and NdeI restrictive sites. Full-length *Xenopus* Ndel1 and NudC were amplified from their ESTs (Thermo Fisher Scientific) and subcloned into pDONR 221 (Invitrogen) plasmid, and then cloned into pDEST17 (Invitrogen) using Gateway (Invitrogen). Preparation of N-terminal fragments of mouse Ndel1 (8–99, 8–192, and 88–192) was described previously (Derewenda et al., 2007). Clones of mNde1$^{7–99}$, mNde1$^{7–170}$ (both gifts from Darkhan Utepbergenov, University of Virginia, Charlottesville, VA), mNde1$^{89–174}$, and mNdel1$^{8–310}$ were generated by subcloning amplified fragments into pHisPar vectors (Sheffield et al., 1999). Clone of 1–174 fragment of mouse Ndel1 in pGEX6P plasmid was a gift from Dr. Andrea Musacchio (European Institute of Oncology, Milan, Italy) and was expressed and purified as described previously (Tarricone et al., 2004). Mutations in the mNdel1 clone were introduced using the QuikChange Mutagenesis kit (Agilent Technologies). Clone of Ran^{Q69L} in pQE32 plasmid was a gift from Dr. Ian Macara (University of Virginia, Charlottesville, VA). Clone of p50/dynamitin was a gift from Dr. Tony Hyman (Max Planck Institute, Dresen, Germany) and the protein was purified as described previously (Wittmann and Hyman, 1999).

Protein purification and antibodies

6-His-tagged *Xenopus* NudC, Nde1 and Ndel1, and rodent Nde1 and Ndel1 proteins were expressed in the *E. coli* strain BL21 (DE3/RIPL; Agilent Technologies), and purified using Ni-NTA resin (QIAGEN) and gel filtration over Superdex 200 (GE Healthcare). For rescue experiments, proteins were dialyzed into 10 mM K-Hepes, 100 mM KCl, pH 7.2–7.8. 6-His-tagged Ran^{Q69L} was expressed in M15 *E. coli* strain (QIAGEN) and purified over Ni-NTA resin. LIS1 protein was a gift from Dr. Andrea Mussachio. 6-His-Ndel1 and 6-His-Nde1 were injected into rabbits to produce polyclonal sera (Covance). Antibodies were affinity purified over immunizing protein coupled to Sepharose beads (GE Healthcare; Harlow and Lane, 1999) and dialyzed into phosphate-buffered saline. Polyclonal antibodies against *Xenopus* Clip170 were published previously (Emanuele et al., 2005). Commercial antibodies included: anti-LIS1 (Abcam), anti-p150^{Glued} (BD), anti-70.1 (Sigma-Aldrich), and anti-tubulin DM1-α (Sigma-Aldrich). An antibody against the dynein intermediate chain (74.1) was a gift from Dr. Kevin Pfister (University of Virginia, Charlottesville, VA).

Circular dichroism measurements

CD spectra of mutated Ndel1 proteins were collected in 100 mM phosphate buffer, 150 mM NaCl, pH 7.0, as described previously (Derewenda et al., 2007).

Xenopus egg extract manipulations and rescue experiments

CSF-arrested (or M phase–arrested) *Xenopus* egg extracts were prepared as described previously (Murray, 1991). Ran asters were assembled by addition of 25 µM constitutively active Ran^{Q69L}. DMSO asters were assembled by addition of 5% tissue culture grade DMSO (Sigma-Aldrich) as described previously (Merlie and Heald, 2001). In some experiments Rhodamine-conjugated tubulin (Cytoskeleton, Inc.) was added to extracts to a final concentration of 15 µg/ml. In function-blocking experiments anti-Ndel1 antibodies were added to a final concentration of 0.5 mg/ml, p50 was added to a final concentration of 1 mg/ml, and anti-70.1 dynein intermediate antibodies (Sigma-Aldrich) were added to final concentration of 1 mg/ml. In protein addition experiments respective proteins were added to CSF-arrested nondepleted extracts containing Rhodamine-labeled tubulin to the final concentration of 100 nM (Nde1 and Ndel1) or 350 nM (LIS1). For rescue experiments either BSA or mNdel1 protein was added to 100 nM final concentration to mock or Ndel1-immunodepleted extracts containing Rhodamine-tubulin (Cytoskeleton, Inc.). In rescue experiments LIS1 was added at 350 nM final concentration. Microtubule nucleation was then induced at 18°C by addition of Ran or DMSO. To quantify aster assay experiments, extracts were treated as indicated for 15 and 30 min at 18°C. For each time point, 1 µl of extract was pipetted into 3 µl of 4% paraformaldehyde fix, squashed under a coverslip, and visualized by fluorescent microscopy as described previously (Murray, 1991). Before quantification both time points were assessed under a fluorescent microscope to determine when focused, mature asters could be detected in control-depleted extracts and microtubule structures at the appropriate time point were quantified as described below. Each grouping of microtubules was classified as either a focused aster or an unfocused structure. 100 microtubule structures were quantified for each condition. Counting was done blind with a similar pattern of coverslip scrolling for each condition. Focused asters indicate clearly focused microtubule structures with star-like morphology. In Ndel1-depleted extracts and some control extracts unfocused microtubules were observed. These microtubules were not distributed uniformly in extracts, but rather came as separated groups of microtubules. One such group would be quantified as an unfocused structure.

In experiments shown in Fig. S4 and Fig. 5 we included additional categories to quantify structures that appear to be intermediates in aster formation as mentioned in the figure legends: hollow asters, multiple foci, and bundles. Hollow asters resemble asters in morphology, but have "hollow" centers. Multiple foci consist of tight microtubule arrays and could be focused as they contain multiple bright spots similar to aster centers, but do not resemble asters in morphology. Bundles are arrays of cross-linked microtubules clearly more bundled than those detected in Ndel1-depleted extracts. All rescue experiments were repeated at least three times. In DMSO addition experiments extracts were fixed after 30 min at 18°C. Because it was impossible to observe separated structures after xNdel1 antibody addition, over 50 fields for each condition were classified as fields with either focused asters or without focused asters.

Embryo staging

Freshly squeezed *Xenopus* eggs were fertilized as described previously (Sive et al., 2000). Developmental stages were evaluated under a stereomicroscope (Stemi 2000-C; Carl Zeiss, Inc.). Embryos were staged according to the normal development table (Nieuwkoop and Faber, 1994). Equal numbers of embryos at each stage collected were harvested in SDS-PAGE loading buffer and analyzed by immunoblotting.

Immunofluorescence

Rhodamine-tubulin Ran asters were fixed for 5 min in 4% paraformaldehyde/30% glycerol/0.1% Triton X-100 in BRB80 and spun through 40% glycerol in a BRB30 cushion at room temperature onto poly-lysine–coated coverglasses (Thermo Fisher Scientific). The cushion was washed and asters postfixed with cold methanol at −20°C for 5 min, then rehydrated with PBST and blocked in 3% BSA/PBST. Primary antibodies were used against DIC (mouse α-70.1, 1:200; Sigma-Aldrich) and Ndel1 (rabbit, 1:1,000). After three washes with PBST secondary antibodies were added (donkey anti–mouse conjugated with FITC 488 nm, 1:400; and donkey anti–rabbit conjugated with Cy5 647 nm, 1:400 [both from Jackson ImmunoResearch Laboratories, Inc.]). After three washes with PBST coverslips were mounted in standard mounting medium and closed with nail polish.

Immunoblotting

For immunoblotting, proteins were resolved using standard SDS-PAGE and transferred to PVDF membrane with a semi-dry transfer apparatus run at 20 V for 60 min. Blots were blocked for 60 min with 3% BSA in phosphate-buffered saline + 0.1% Tween 20 (PBST) or 5% milk in Tris-buffered saline + 0.1% Tween 20 (TBST), incubated with primary antibodies diluted into 3% BSA in PBST/5% milk in TBST, washed four times for 5 min with PBST/TBST, and blocked again for 30 min before incubation with secondary antibody. Anti–rabbit or anti–mouse secondary antibodies conjugated with horseradish peroxidase (Jackson ImmunoResearch Laboratories, Inc.) were used at 1:10,000. Blots were washed with PBST or TBST as before, briefly rinsed with PBS or TBS, and developed with the ECL reagent (GE Healthcare; Thermo Fisher Scientific) on x-ray film (Kodak). Primary antibodies used for immunoblotting included: anti-Nde1 (1:5,000), anti-Ndel1 (1:5,000–1:10,000), anti-LIS1 (1:2,500), anti-$p150^{Glued}$ (1:2,000), anti-74.1 (1:2,000), and anti-Clip170 (1:2,000). To analyze amounts of tubulin in microtubule pelleting assays, samples were diluted 20-fold and α-tubulin DMIα antibody was used at 1:5,000.

Immunoprecipitation and immunodepletion

Immunoprecipitations were performed with 60 µg affinity-purified α-Ndel1 antibodies DMP-coupled to 20 µl of Affi-prep Protein A beads (Bio-Rad Laboratories) and repeated twice. Immunoprecipitates were washed off the beads with 100 mM glycine, pH 2.3, TCA precipitated, separated by a standard SDS-PAGE, and immunoblotted as indicated. For immunodepletion and rescue of *Xenopus* extracts, 60 µg of mock rabbit IgG (Sigma-Aldrich) or affinity-purified rabbit anti-xNdel1 antibody was bound to 50 µl of Dynal magnetic beads (Invitrogen) per 100 µl CSF extract immunodepletion. Depletions were performed with two rounds of fresh beads, each time for 30 min on ice.

Microtubule pelleting

Microtubules were formed in CSF-arrested extracts by addition of 25 mM Ran^{Q69L} for 30 min. Reactions were resuspended in 30% glycerol in BRB80, loaded onto 40% glycerol in BRB80, and centrifuged in a rotor (model S120-AT2; Sorvall) at 42,000 rpm at 22°C. Cushions were washed with BRB80 and pellets were analyzed by immunoblot.

Pull-downs

For pull-down experiments, 30 µM proteins were dialyzed into a binding buffer (100 mM $NaHCO_3$ and 500 mM NaCl, pH 8.3) and incubated with HCl-washed Sepharose CNBr-activated beads for 1–2 h at room temperature. Beads were washed three times with binding buffer, blocked with 100 mM Tris, pH 8.0, for 1.5 h at room temperature, and washed with PBS. After incubation with CSF-arrested extracts beads were washed five times with CSF-XB + 0.1% Triton X-100. In some experiments additional NaCl was added to the wash buffer as indicated in figure legends. Beads were separated on SDS-PAGE and analyzed by immunoblotting. All pull-down experiments were repeated at least three times, except for the wash-off experiment, which was repeated once.

Microscopy

Fixed asters were photographed at room temperature using a spinning disk confocal imaging system with a 63x 1.4 NA Plan-Apochromat objective lens covered with immersion oil (Carl Zeiss, Inc.). The inverted microscope (Axiovert 200; Carl Zeiss, Inc.) with a confocal attachment (PerkinElmer) and a krypton/argon laser (PerkinElmer) with AOTF control was used to detect illumination at 488, 568, or 647 nm. Images in Fig.1 and Fig. 2 d were obtained with a Digital CCD camera (Hamamatsu Photonics). Image acquisition, shutters, and z-slices were all controlled by UltraView RS imaging software (PerkinElmer). Z-series optical overlapping sections were obtained in 0.4-µm steps. Digital images for experiments in Fig. 2 b, Figs. 3–5, and the supplemental figures were taken with a cooled 14-bit frame transfer camera (EMCCD C9100-50; Hamamatsu Photonics). Image acquisition, shutters, and z-slices were all controlled by Volocity imaging software (PerkinElmer). All images compared were taken under identical conditions, and were scaled identically. Contrast was adjusted in Photoshop (Adobe) identically for all images compared.

Online supplemental material

Fig. S1 shows additional characterization of anti-xNde1 and anti-xNdel1 antibodies, and expression levels of both proteins during frog development. Fig. S2 shows the effect of anti-xNdel1 antibodies on microtubule nucleation and formation of DMSO asters. Fig. S3 shows Coomassie gels of recombinant proteins used in this study and CD spectroscopy of newly characterized mutations in $mNdel1^{8–192}$ variants to confirm their proper folding. Fig. S4 shows the effect of recombinant protein additions on Ran aster formation in nondepleted extracts. Fig. S5 shows additional characterization of the newly identified dynein-binding site in the N terminus of Ndel1. Online supplemental material is available at http://www.jcb.org/cgi/content/full/jcb.201011142/DC1.

We thank Dr. Andrea Musacchio for LIS1 protein and plasmids. We also thank Drs. Ian Macara and Tony Hyman for plasmids, Dr. Kevin Pfister for anti-74.1 dynein intermediate chain antibodies, Darkhan Utepbergenov for Nde1 plasmids and proteins, and Dr. Dan Burke (University of Virginia, Charlottesville, VA) for critical reading of the manuscript.

This work was supported by a grant from the National Institutes of Health (R01-NS036267).

Submitted: 29 November 2010
Accepted: 4 January 2011

References

Bradshaw, N.J., S. Christie, D.C. Soares, B.C. Carlyle, D.J. Porteous, and J.K. Millar. 2009. NDE1 and NDEL1: multimerisation, alternate splicing and DISC1 interaction. *Neurosci. Lett.* 449:228–233. doi:10.1016/j.neulet.2008.10.095

Burgess, S.A., M.L. Walker, H. Sakakibara, P.J. Knight, and K. Oiwa. 2003. Dynein structure and power stroke. *Nature.* 421:715–718. doi:10.1038/nature01377

Collins, D.M., H. Murdoch, A.J. Dunlop, E. Charych, G.S. Baillie, Q. Wang, F.W. Herberg, N. Brandon, A. Prinz, and M.D. Houslay. 2008. Ndel1 alters its conformation by sequestering cAMP-specific phosphodiesterase-4D3 (PDE4D3) in a manner that is dynamically regulated through Protein Kinase A (PKA). *Cell. Signal.* 20:2356–2369. doi:10.1016/j.cellsig.2008.09.017

Derewenda, U., C. Tarricone, W.C. Choi, D.R. Cooper, S. Lukasik, F. Perrina, A. Tripathy, M.H. Kim, D.S. Cafiso, A. Musacchio, and Z.S. Derewenda. 2007. The structure of the coiled-coil domain of Ndel1 and the basis of its interaction with Lis1, the causal protein of Miller-Dieker lissencephaly. *Structure.* 15:1467–1481. doi:10.1016/j.str.2007.09.015

Efimov, V.P., and N.R. Morris. 2000. The LIS1-related NUDF protein of *Aspergillus nidulans* interacts with the coiled-coil domain of the NUDE/RO11 protein. *J. Cell Biol.* 150:681–688. doi:10.1083/jcb.150.3.681

Emanuele, M.J., M.L. McCleland, D.L. Satinover, and P.T. Stukenberg. 2005. Measuring the stoichiometry and physical interactions between components elucidates the architecture of the vertebrate kinetochore. *Mol. Biol. Cell.* 16:4882–4892. doi: 10.1091/mbc.E05-03-0239

Feng, Y., E.C. Olson, P.T. Stukenberg, L.A. Flanagan, M.W. Kirschner, and C.A. Walsh. 2000. LIS1 regulates CNS lamination by interacting with mNudE, a central component of the centrosome. *Neuron.* 28:665–679. doi:10.1016/S0896-6273(00)00145-8

Gaglio, T., M.A. Dionne, and D.A. Compton. 1997. Mitotic spindle poles are organized by structural and motor proteins in addition to centrosomes. *J. Cell Biol.* 138:1055–1066. doi:10.1083/jcb.138.5.1055

Goshima, G., F. Nédélec, and R.D. Vale. 2005. Mechanisms for focusing mitotic spindle poles by minus end-directed motor proteins. *J. Cell Biol.* 171:229–240. doi:10.1083/jcb.200505107

Harlow, E., and D. Lane. 1999. Using Antibodies: A Laboratory Manual. Cold Spring Harbor Laboratory Press, Cold Spring Harbor, NY. 495 pp.

Heald, R., R. Tournebize, T. Blank, R. Sandaltzopoulos, P. Becker, A. Hyman, and E. Karsenti. 1996. Self-organization of microtubules into bipolar spindles around artificial chromosomes in *Xenopus* egg extracts. *Nature.* 382:420–425. doi:10.1038/382420a0

Kalab, P., R.T. Pu, and M. Dasso. 1999. The ran GTPase regulates mitotic spindle assembly. *Curr. Biol.* 9:481–484. doi:10.1016/S0960-9822(99)80213-9

Kim, M.H., D.R. Cooper, A. Oleksy, Y. Devedjiev, U. Derewenda, O. Reiner, J. Otlewski, and Z.S. Derewenda. 2004. The structure of the N-terminal domain of the product of the lissencephaly gene Lis1 and its functional implications. *Structure.* 12:987–998. doi:10.1016/j.str.2004.03.024

Liang, Y., W. Yu, Y. Li, Z. Yang, X. Yan, Q. Huang, and X. Zhu. 2004. Nudel functions in membrane traffic mainly through association with Lis1 and cytoplasmic dynein. *J. Cell Biol.* 164:557–566. doi:10.1083/jcb.200308058

Liang, Y., W. Yu, Y. Li, L. Yu, Q. Zhang, F. Wang, Z. Yang, J. Du, Q. Huang, X. Yao, and X. Zhu. 2007. Nudel modulates kinetochore association and function of cytoplasmic dynein in M phase. *Mol. Biol. Cell.* 18:2656–2666. doi:10.1091/mbc.E06-04-0345

Ma, L., M.Y. Tsai, S. Wang, B. Lu, R. Chen, J.R. Iii, X. Zhu, and Y. Zheng. 2009. Requirement for Nudel and dynein for assembly of the lamin B spindle matrix. *Nat. Cell Biol.* 11:247–256. doi:10.1038/ncb1832

Mateja, A., T. Cierpicki, M. Paduch, Z.S. Derewenda, and J. Otlewski. 2006. The dimerization mechanism of LIS1 and its implication for proteins containing the LisH motif. *J. Mol. Biol.* 357:621–631. doi:10.1016/j.jmb.2006.01.002

McKenney, R.J., M. Vershinin, A. Kunwar, R.B. Vallee, and S.P. Gross. 2010. LIS1 and NudE induce a persistent dynein force-producing state. *Cell.* 141:304–314. doi:10.1016/j.cell.2010.02.035

Merdes, A., R. Heald, K. Samejima, W.C. Earnshaw, and D.W. Cleveland. 2000. Formation of spindle poles by dynein/dynactin-dependent transport of NuMA. *J. Cell Biol.* 149:851–862. doi:10.1083/jcb.149.4.851

Merlie, J. Jr., and R. Heald. 2001. Mitotic spindle assembly in vitro. *Curr. Protoc. Cell Biol*. Chapter 11:Unit 11 13.

Mizuno, N., A. Narita, T. Kon, K. Sutoh, and M. Kikkawa. 2007. Three-dimensional structure of cytoplasmic dynein bound to microtubules. *Proc. Natl. Acad. Sci. USA.* 104:20832–20837. doi:10.1073/pnas.0710406105

Mori, D., Y. Yano, K. Toyo-oka, N. Yoshida, M. Yamada, M. Muramatsu, D. Zhang, H. Saya, Y.Y. Toyoshima, K. Kinoshita, et al. 2007. NDEL1 phosphorylation by Aurora-A kinase is essential for centrosomal maturation, separation, and TACC3 recruitment. *Mol. Cell. Biol.* 27:352–367. doi:10.1128/MCB.00878-06

Mori, D., M. Yamada, Y. Mimori-Kiyosue, Y. Shirai, A. Suzuki, S. Ohno, H. Saya, A. Wynshaw-Boris, and S. Hirotsune. 2009. An essential role of the aPKC-Aurora A-NDEL1 pathway in neurite elongation by modulation of microtubule dynamics. *Nat. Cell Biol.* 11:1057–1068. doi:10.1038/ncb1919

Murray, A.W. 1991. Cell cycle extracts. *Methods Cell Biol.* 36:581–605. doi:10.1016/S0091-679X(08)60298-8

Niethammer, M., D.S. Smith, R. Ayala, J. Peng, J. Ko, M.S. Lee, M. Morabito, and L.H. Tsai. 2000. NUDEL is a novel Cdk5 substrate that associates with LIS1 and cytoplasmic dynein. *Neuron.* 28:697–711. doi:10.1016/S0896-6273(00)00147-1

Nieuwkoop, P.D., and J. Faber. 1994. Normal table of *Xenopus laevis* (Daudin): A systematical and chronological survey of the development from the fertilized egg till the end of metamorphosis. Garland Pub., NY. 252 pp.

Ohba, T., M. Nakamura, H. Nishitani, and T. Nishimoto. 1999. Self-organization of microtubule asters induced in *Xenopus* egg extracts by GTP-bound Ran. *Science.* 284:1356–1358. doi:10.1126/science.284.5418.1356

Sasaki, S., A. Shionoya, M. Ishida, M.J. Gambello, J. Yingling, A. Wynshaw-Boris, and S. Hirotsune. 2000. A LIS1/NUDEL/cytoplasmic dynein heavy chain complex in the developing and adult nervous system. *Neuron.* 28:681–696. doi:10.1016/S0896-6273(00)00146-X

Schroer, T.A. 2004. Dynactin. *Annu. Rev. Cell Dev. Biol.* 20:759–779. doi:10.1146/annurev.cellbio.20.012103.094623

Sheffield, P., S. Garrard, and Z. Derewenda. 1999. Overcoming expression and purification problems of RhoGDI using a family of "parallel" expression vectors. *Protein Expr. Purif.* 15:34–39. doi:10.1006/prep.1998.1003

Sive, H.L., R.M. Grainger, and R.M. Harland. 2000. Early Development of *Xenopus laevis*: A Laboratory Manual. Cold Spring Harbor Laboratory Press, Cold Spring Harbor, NY. 338 pp.

Smith, D.S., M. Niethammer, R. Ayala, Y. Zhou, M.J. Gambello, A. Wynshaw-Boris, and L.H. Tsai. 2000. Regulation of cytoplasmic dynein behaviour and microtubule organization by mammalian Lis1. *Nat. Cell Biol.* 2:767–775. doi:10.1038/35041000

Stehman, S.A., Y. Chen, R.J. McKenney, and R.B. Vallee. 2007. NudE and NudEL are required for mitotic progression and are involved in dynein recruitment to kinetochores. *J. Cell Biol.* 178:583–594. doi:10.1083/jcb.200610112

Stukenberg, P.T., K.D. Lustig, T.J. McGarry, R.W. King, J. Kuang, and M.W. Kirschner. 1997. Systematic identification of mitotic phosphoproteins. *Curr. Biol.* 7:338–348. doi:10.1016/S0960-9822(06)00157-6

Tai, C.Y., D.L. Dujardin, N.E. Faulkner, and R.B. Vallee. 2002. Role of dynein, dynactin, and CLIP-170 interactions in LIS1 kinetochore function. *J. Cell Biol.* 156:959–968. doi:10.1083/jcb.200109046

Tarricone, C., F. Perrina, S. Monzani, L. Massimiliano, M.H. Kim, Z.S. Derewenda, S. Knapp, L.H. Tsai, and A. Musacchio. 2004. Coupling PAF signaling to dynein regulation: structure of LIS1 in complex with PAF-acetylhydrolase. *Neuron.* 44:809–821.

Vaisberg, E.A., M.P. Koonce, and J.R. McIntosh. 1993. Cytoplasmic dynein plays a role in mammalian mitotic spindle formation. *J. Cell Biol.* 123:849–858. doi:10.1083/jcb.123.4.849

Vergnolle, M.A., and S.S. Taylor. 2007. Cenp-F links kinetochores to Ndel1/Nde1/Lis1/dynein microtubule motor complexes. *Curr. Biol.* 17:1173–1179. doi:10.1016/j.cub.2007.05.077

Walczak, C.E., and R. Heald. 2008. Mechanisms of mitotic spindle assembly and function. *Int. Rev. Cytol.* 265:111–158. doi:10.1016/S0074-7696(07)65003-7

Walczak, C.E., I. Vernos, T.J. Mitchison, E. Karsenti, and R. Heald. 1998. A model for the proposed roles of different microtubule-based motor proteins in establishing spindle bipolarity. *Curr. Biol.* 8:903–913. doi:10.1016/S0960-9822(07)00370-3

Wang, S., and Y. Zheng. 2011. Identification of a novel Dynein binding domain in nudel essential for spindle pole organization in *Xenopus* egg extract. *J. Biol. Chem.* 286:587–593. doi:10.1074/jbc.M110.181578

Wilde, A., and Y. Zheng. 1999. Stimulation of microtubule aster formation and spindle assembly by the small GTPase Ran. *Science.* 284:1359–1362. doi:10.1126/science.284.5418.1359

Wittmann, T., and T. Hyman. 1999. Recombinant p50/dynamitin as a tool to examine the role of dynactin in intracellular processes. *Methods Cell Biol.* 61:137–143. doi:10.1016/S0091-679X(08)61978-0

Xiang, X., A.H. Osmani, S.A. Osmani, M. Xin, and N.R. Morris. 1995. NudF, a nuclear migration gene in *Aspergillus nidulans*, is similar to the human *LIS-1* gene required for neuronal migration. *Mol. Biol. Cell.* 6:297–310.

Yan, X., F. Li, Y. Liang, Y. Shen, X. Zhao, Q. Huang, and X. Zhu. 2003. Human Nudel and NudE as regulators of cytoplasmic dynein in poleward protein transport along the mitotic spindle. *Mol. Cell. Biol.* 23:1239–1250. doi:10.1128/MCB.23.4.1239-1250.2003